Studying of the Covid-19 model by using the finite element method: Theoretical and numerical simulation

Weaam Alhejili
Princess Noura Bint AbdulRahman University: Princess Nourah bint Abdulrahman University
M. M. Khader
Imam Muhammad bin Saud Islamic University: Imam Muhammad Ibn Saud Islamic University
khaled lotfy (khlotfy_1@yahoo.com)
Zagazig University Faculty of Science https://orcid.org/0000-0001-9383-1361
A. El-Bary
Arab Academy for Science Technology and Maritime Transport
M. Adel
Cairo University Faculty of Science

Research Article

Keywords: Covid-19, FEM, Optimization technique, Residual error function, RK4 method

Posted Date: May 25th, 2023

DOI: https://doi.org/10.21203/rs.3.rs-2733047/v1

Version of Record: A version of this preprint was published at Soft Computing on October 19th, 2023. See the published version at https://doi.org/10.1007/s00500-023-09310-6.

Studying of the Covid-19 model by using the finite element method: Theoretical and numerical simulation

W. Alhejili[1], M. M. Khader[2,3], K. Lotfy[4,5], A. A. El-Bary[6,7] and M. Adel[8,9]

[1]Department of Mathematical Sciences, College of Science, Princess Nourah bint Abdulrahman University, P.O. Box 84428, Riyadh 11671, Saudi Arabia

[2]Department of Mathematics, Faculty of Science, Benha University, Benha, Egypt

[3]Department of Mathematics and Statistics, College of Science, Imam Mohammad Ibn Saud Islamic University (IMSIU), Riyadh: 11566, Saudi Arabia

[4]4Department of Mathematics, Faculty of Science, Zagazig University, Zagazig, Egypt

[5]5Department of Mathematics, Faculty of Science, Taibah University, Medina, Saudi Arabia

[6]Arab Academy for Science, Technology and Maritime Transport, P.O. Box 1029, Alexandria, Egypt

[7]7Council of future studies and risk management, Academy of Sci. Res. and Tech., Cairo, Egypt

[8]Department of Mathematics, Faculty of Science, Islamic University of Madinah, Medina, KSA

[9]Department of Mathematics, Faculty of Science, Cairo University, Giza, Egypt

[1]waalhejali@pnu.edu.sa, [2]mmkhader@imamu.edu.sa, [4]khlotfy@zu.edu.eg, [6]aaelbary@aast.edu, [8]adel@sci.cu.edu.eg, [9]mohammedadel@cu.edu.eg

Abstract

This study simulates the start of coronavirus infection using a mathematical model based on ordinary differential equations (Covid-19). Additionally, provide the numerical treatment and simulation of this model using the finite element approach (FEM). The goal of this research is to stop and slow the spread of a sickness that is ravaging the globe. A susceptible person may also transfer immediately to the quarantined class after the exposed person has been quarantined or moved to one of the contaminated classes. This model was employed by the researchers to account for both asymptomatic and symptomatic infected people. The proposed model is reduced to a set of algebraic equations using the FEM. The resulting system is then created as an optimization problem with constraints, which is subsequently optimized to obtain the solution and the unknown coefficients. The obtained findings are compared to those produced using the fourth-order Runge-Kutta method (RK4). Finally, we calculate the residual error function of the approximation in order to validate the FEM, and it is presented in symmetric forms.

Keywords: Covid-19; FEM; Optimization technique; Residual error function; RK4 method.

MSC 2010: 34A12; 41A30; 47H10; 65N20.

1 Introduction

There are many models were used to describe many phenomena in biology and Covid-19 like([1]-[4]), In order to gain insight into the pandemic's mode of spread, transmission, effect, prevention,

and control, as well as the effects of preventive measures like hand washing with a disinfectant like hand sanitizer, increasing distance between people, and face masks for everyone, researchers have been using and creating mathematical models ([5]-[7]).
In ([5], [8]), the early stages of the outbreak scenario of Covid-19's dissemination in Nigeria were examined and assessed by the authors. Good research on preventive and therapeutic strategies to curb the epidemic has been provided by researchers from a range of fields, with encouraging outcomes. The most current models need to be examined more thoroughly, nevertheless, in order to make a valid and satisfied judgment.

All of the models described in the preceding investigations used classical derivatives, with some restrictions on the order of differential equations involved ([9], [10]). These differential operators have memory qualities, allowing them to be utilized to demonstrate a wide range of scientific phenomena and facts involving dynamics ([11]-[17]). The concept of differential equations in general, and ODEs in particular, has gained a lot of interest due to its wide-ranging improvements and numerous applications in several disciplines ([18]-[22]).

Many academics have successfully used a variety of numerical and approximation approaches to solve ODEs. When dealing with this kind of issue, the finite element approach (FEM) [14] has a number of benefits because the coefficients for the solution can be quickly acquired using any of the available numerical programs. In the paragraphs that follow, we'll go through this method's primary benefits:

1. FEM may be used to model and solve irregular and complicated geometrical shapes.

2. FEM may be used to solve a problem with great precision and efficiency.

3. For some time-dependent simulations, such crash simulations, where deformations in one area depend on deformations in another, FEM is more advantageous.

The primary goal of this study is to numerically solve the Covid-19 suggested system. The FEM breaks down the issue into a series of algebraic equations. The system is then modeled as a restricted optimization problem, which is subsequently optimized to find the solution and the unknown coefficients. By examining the locally asymptotically stable disease-free equilibrium, the locally asymptotically stable endemic equilibrium point, and the globally asymptotically stable endemic equilibrium, the recommended model's qualitative analysis is provided.
The following is how the paper is set up:

- The model is formulated and the parameters defined in the model are described in Section 2.

- We provide a qualitative analysis of the suggested model in Section 3.

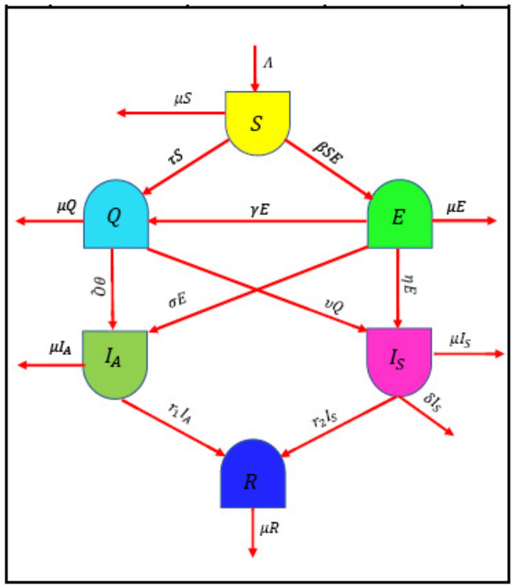

Figure 1. Flowchart describing the dynamics of spread the model of Covid-19.

- The FEM solution approach is shown in Section 4.
- The model's sensitivity analysis and numerical simulation are highlighted in Section 5.
- The paper's conclusion is presented in Section 6.

2 Formulation of the Model

Let $N(t)$ be the total number of people. Individuals who are susceptible $S(t)$, exposed $E(t)$, asymptotically infected $I_A(t)$, symptomatically infected $I_S(t)$, quarantined $Q(t)$, and removed $R(t)$ from Covid-19 The seven classifications in this population are $R(t)$.
Taking this into account, the total population is [23]

$$N(t) = S(t) + E(t) + Q(t) + I_A(t) + I_S(t) + R(t).$$

A system of ODEs is generated using the schematic diagram in Figure 1 and described in [23]: The nonlinear ordinary differential equations system can be written as follows:

$$
\begin{aligned}
&\dot{S}(t)=\Lambda-(\tau+\mu)S(t)-\beta S(t)E(t),\\
&\dot{E}(t)=\beta S(t)E(t)-(\gamma+\mu+\eta+\sigma)E(t),\\
&\dot{Q}(t)=\tau S(t)+\gamma E(t)-(\mu+v+\theta)Q(t),\\
&\dot{I}_A(t)=\sigma E(t)+\theta Q(t)-(\mu+r_1)\,I_A(t),\\
&\dot{I}_S(t)=\eta E(t)+vQ(t)-(\delta+\mu+r_2)\,I_S(t),\\
&\dot{R}(t)=r_1 I_A(t)+r_2 I_S(t)-\mu R(t),
\end{aligned}
\tag{1}
$$

with the following initial conditions:

$$
S(0)=S_0,\qquad E(0)=E_0,\qquad Q(0)=Q_0,\qquad I_A(0)=IA_0,\qquad I_S(0)=IS_0,\qquad R(0)=R_0, \tag{2}
$$

all the quantities S_0, E_0, Q_0, IA_0, IS_0, $R_0 \geq 0$. Where included parameters are defined in details in [23].

3 The proposed model's qualitative analysis

Because the reproduction number is required for the investigation of infection illness models, we give the computation and presentation of the basic reproduction number [24] in this section. We also present the invariant region for the suggested model (1) and investigate the following points:

1. Its disease-free equilibrium is locally asymptotically stable.
2. One-of-a-kind endemic equilibrium point.
3. Its one-of-a-kind endemic equilibrium point is locally asymptotically stable.
4. Its endemic equilibrium is globally asymptotically stable.

3.1 Region of invariance

It is crucial to note that $S(t), E(t), Q(t), I_A(t), I_S(t), R(t)$ are nonnegative for all $t \geq 0$ which is important for characterizing the human population in the model (1). This guarantees that the system's solution (1) with positive initial data remains positive for all $t \geq 0$ and is bounded. It is easy to see that:

$$
\frac{dN(t)}{dt}=\Lambda-\mu N(t)-\delta I_S(t),\ \text{and}\ \sup_{t\to+\infty} N(t)\leqslant\frac{\Lambda}{\mu}.
$$

Taking these assumptions into account, we can investigate this model in the region:

$$
\Omega=\left\{(S(t),E(t),Q(t),I_A(t),I_S(t),R(t))\in\mathbb{R}_+^6:\quad 0\leqslant N(t)\leqslant\frac{\Lambda}{\mu}\right\}. \tag{3}
$$

Now, we can see that the system under study (1) is epidemiologically well-posed, and that all of its componds $(S(t), E(t), Q(t), I_A(t), I_S(t), R(t)) \in \mathbb{R}_+^6$ remain in Ω are well-posed as well (ref3).

3.2 Diseases free equilibrium point

We set $E = Q = I_A = I_S = R = 0$ to achieve the disease free equilibrium (DFE), i.e. the DFE point $\bar{\mathbf{E}}_0$ of the system (1) can be defined as follows:

$$\bar{\mathbf{E}}_0 = (S_0, 0, 0, 0, 0, 0) = \left(\frac{\Lambda}{\tau + \mu}, 0, 0, 0, 0, 0\right).$$

Definition 1. The expected value of infection rate per time unit is given by $\mathfrak{R}_0$, the fundamental reproduction number.

The major goal of this section is to deduce the condition that makes the $\bar{\mathbf{E}}_0$ asymptotically stable locally. There are some facts [24] will help us reach this goal.

The article develops an equation that involves the classes of the exposed population without symptom, and infected population with symptom as follows, without losing generality, as shown by the model (1) [23]:

$$\begin{aligned}
\dot{E}(t) &= \beta S(t)E(t) - (\gamma + \mu + \eta + \sigma)E(t),\\
\dot{Q}(t) &= \tau S(t) + \gamma E(t) - (\mu + v + \theta)Q(t),\\
\dot{I}_A(t) &= \sigma E(t) + \theta Q(t) - (\mu + r_1)\, I_A(t),\\
\dot{I}_S(t) &= \eta E(t) + vQ(t) - (\delta + \mu + r_2)\, I_S(t).
\end{aligned} \tag{4}$$

We may create the following matrices $\mathfrak{F}$ and $\mathfrak{V}$ using equations (ref4) and the same technique used in [23]:

$$\mathfrak{F} = \begin{pmatrix} \beta S(t)E(t) \\ 0 \\ 0 \\ 0 \end{pmatrix}, \qquad \mathfrak{V} = \begin{pmatrix} (\gamma + \mu + \eta + \sigma)E(t) \\ -\tau S(t) - \gamma E(t) + (\mu + v + \theta)Q(t) \\ -\sigma E(t) - \theta Q(t) + (\mu + r_1)\, I_A(t) \\ -\eta E(t) - vQ(t) + (\delta + \mu + r_2)\, I_S(t) \end{pmatrix}.$$

As did in [23], the Jacobian matrix of $\mathfrak{F}$ and $\mathfrak{V}$ at $\bar{\mathbf{E}}_0$, denoted by F and V, respectively are:

$$F = \begin{pmatrix} \frac{\beta\Lambda}{\tau+\mu} & 0 & 0 & 0 \\ 0 & 0 & 0 & 0 \\ 0 & 0 & 0 & 0 \\ 0 & 0 & 0 & 0 \end{pmatrix}, \qquad V = \begin{pmatrix} \gamma + \mu + \eta + \sigma & 0 & 0 & 0 \\ -\gamma & \mu + v + \theta & 0 & 0 \\ -\sigma & -\theta & \mu + r_1 & 0 \\ -\eta & -v & 0 & \delta + \mu + r_2 \end{pmatrix}.$$

Also, as did in [24], $\mathfrak{R}_0$ is defined by:

$$\mathfrak{R}_0 = \rho\left(FV^{-1}\right) = \frac{\beta\Lambda}{(\gamma + \mu + \eta + \sigma)(\tau + \mu)} > 0,$$

where ρ refers for spectral radius of

$$FV^{-1} = \begin{pmatrix} \frac{\beta\Lambda}{A(\tau+\mu)} & 0 & 0 & 0 \\ 0 & 0 & 0 & 0 \\ 0 & 0 & 0 & 0 \\ 0 & 0 & 0 & 0 \end{pmatrix}.$$

Theorem 1. ***(A study of the $\bar{\mathbf{E}}_0$'s local stability** [23])*

If $\mathfrak{R}_0 < 1$, the disease-free equilibrium $\bar{\mathbf{E}}_0$ is locally asymptotically stable.

3.3 Analysis of the existence and stability of an endemic equilibrium point

The existence of an endemic equilibrium point, indicated by $\bar{\mathbf{E}}_1 = (S^*,\ E^*,\ Q^*, I_A^*,\ I_S^*,\ R^*)$, will be discussed in this part. The following notions will be used: $S(t) = S$, $E(t) = E$, $Q(t) = Q$, $I_A(t) = I_A$, $I_S(t) = I_S$, and $R(t) = R$.
This endemic equilibrium is known to satisfy [23]:

$$\begin{aligned} 0 &= \Lambda - (\tau+\mu)S^* - \beta S^* E^*, \\ 0 &= \beta S^* E^* - (\gamma+\mu+\eta+\sigma)E^*, \\ 0 &= \tau S^* + \gamma E^* - (\mu+v+\theta)Q^*, \\ 0 &= \sigma E^* + \theta Q^* - (\mu+r_1)\, I_A^*, \\ 0 &= \eta E^* + v Q^* - (\delta+\mu+r_2)\, I_S^*, \\ 0 &= r_1 I_A^* + r_2 I_S^* - \mu R^*. \end{aligned} \tag{5}$$

We can find the solution of this system (5) in the following way using basic computation and simplification [23]:

$$S^\star = \frac{\gamma+\mu+\eta+\sigma}{\beta}, \qquad E^\star = \frac{(\tau+\mu)}{\beta}\left(\mathfrak{R}_0 - 1\right),$$

$$Q^* = \frac{\tau\beta(\gamma+\mu+\eta+\sigma) + \gamma(\tau+\mu)}{\beta(\mu+v+\theta)}\left(\mathfrak{R}_0 - 1\right),$$

$$I_A^\star = \frac{(\tau+\mu)[\sigma(\mu+v+\theta)+\gamma\theta]}{\beta(\mu+v+\theta)\,(\mu+r_1)}\left(\mathfrak{R}_0 - 1\right),$$

$$I_S^\star = \frac{(\tau+\mu)[\eta(\mu+v+\theta)+\tau\beta v(\gamma+v+\eta+\sigma)+\gamma]}{\beta(\mu+v+\theta)\,(\delta+\mu+r_2)}\left(\mathfrak{R}_0 - 1\right),$$

$$\begin{aligned} R^* =& \frac{1}{\mu}\left[\frac{[(\tau+\mu)[\sigma(\mu+v+\theta)+\gamma\theta]]r_1}{\beta(\mu+v+\theta)\,(\mu+r_1)}\right. \\ &\left. + \frac{[(\tau+\mu)[\eta(\mu+v+\theta)+\tau\beta v(\gamma+v+\eta+\sigma)+\gamma]]r_2}{\beta(\mu+v+\theta)\,(\delta+\mu+r_2)}\right]\left(\mathfrak{R}_0 - 1\right). \end{aligned}$$

We can express and prove the following theorem in view of these components of the system solution (5).

Theorem 2. *[23]*

The system (1) has a single endemic equilibrium point, which is defined as:

$$\bar{\mathbf{E}}_1 = \left(\frac{\gamma + \mu + \eta + \sigma}{\beta}, a\left(\mathfrak{R}_0 - 1\right), b\left(\mathfrak{R}_0 - 1\right), c\left(\mathfrak{R}_0 - 1\right), d\left(\mathfrak{R}_0 - 1\right), \frac{(cr_1 + dr_2)}{\mu}\left(\mathfrak{R}_0 - 1\right) \right),$$

whenever $\mathfrak{R}_0 > 1$ and

$$a = \frac{(\tau + \mu)}{\beta}, \qquad b = \frac{\tau\beta(\gamma + \mu + \eta + \sigma) + \gamma(\tau + \mu)}{\beta(\mu + v + \theta)},$$

$$c = \frac{(\tau + \mu)[\sigma(\mu + v + \theta) + \gamma\theta]}{\beta(\mu + v + \theta)\left(\mu + r_1\right)}, \qquad d = \frac{(\tau + \mu)[\eta(\mu + v + \theta) + \tau\beta v(\gamma + v + \eta + \sigma) + \gamma]}{\beta(\mu + v + \theta)\left(\delta + \mu + r_2\right)}.$$

Theorem 3. ***(A study of the $\bar{E}_1$'s local stability** [23])*

The endemic equilibrium $\bar{\mathbf{E}}_1$ is locally asymptotically stable if $\mathfrak{R}_0 > 1$.

Theorem 4.

There are no periodic orbits in the system (1).
Because Ω is positively invariant, all solutions of the system (1) originate and remain in Ω for all t, according to the Poincare-Bendixson theorem. As a result, we'll wrap up this impoetant note with the following theorem.

Theorem 5. ***(A study of the $\bar{E}_1$'s global stability** [23])*

When $\mathfrak{R}_0 > 1$, the system (1)'s endemic equilibrium $\bar{\mathbf{E}}_1$ is globally asymptotically stable. The endemic equilibrium for the system (1) is globally asymptotically stable whenever.

4 FEM solution procedure

The FEM is a strong approach for solving ODEs and PDEs as well as integral equations. The primary concept behind this approach is that the entire domain is broken into smaller, finite-dimensional elements known as Finite Elements. It is a numerical technique used in current engineering analysis to investigate many problems in domains such as chemical processing [15], solid mechanics [25], fluid mechanics [26], heat transfer [27], electrical systems, and many others. The following steps will be followed in order to apply the FEM [16]:

1. The suggested system's variational formulation.

2. Discrete-element discretization, which is a method of discretizing using finite elements.
3. The creation of element equations.
4. Putting together the element equations.
5. Boundary conditions are imposed.
6. Solve an algebraic system of equations.

In the subsections that follow, we'll put these steps into practice.

4.1 Variational formulation of the system (1)

Over a typical linear element (t_e, t_{e+1}), the related variational form of the system of Eqs.(1) is as follows:

$$\int_{t_e}^{t_{e+1}} \phi_1 \left[S'(t) - \Lambda + (\tau + \mu)S(t) + \beta S(t)E(t)\right] dt = 0, \tag{6}$$

$$\int_{t_e}^{t_{e+1}} \phi_2 \left[E'(t) - \beta S(t)E(t) + (\gamma + \mu + \eta + \sigma)E(t)\right] dt = 0, \tag{7}$$

$$\int_{t_e}^{t_{e+1}} \phi_3 \left[Q'(t) - \tau S(t) - \gamma E(t) + (\mu + v + \theta)Q(t)\right] dt = 0 \tag{8}$$

$$\int_{t_e}^{t_{e+1}} \phi_4 \left[I_A'(t) - \sigma E(t) - \theta Q(t) + (\mu + r_1)\, I_A(t)\right] dt = 0, \tag{9}$$

$$\int_{t_e}^{t_{e+1}} \phi_5 \left[I_S'(t) - \eta E(t) - vQ(t) + (\delta - \mu - r_2)\, I_S(t)\right] dt = 0, \tag{10}$$

$$\int_{t_e}^{t_{e+1}} \phi_6 \left[R'(t) - r_1 I_A(t) - r_2 I_S(t) + \mu R(t)\right] dt = 0, \tag{11}$$

where ϕ_1, ϕ_2, ϕ_3, ϕ_4, ϕ_5, and ϕ_6 are arbitrary test functions that can be thought of as variations in $S(t)$, $E(t), Q(t)$, $I_A(t)$, $I_S(t)$ and $R(t)$, respectively.

4.2 Model's finite element formulation

The domain is discretized when it is split up into a finite number of smaller domains. The term "element" is used to describe each sub-domain. A group of elements make up the finite-element mesh. The variational formulation of the given problem is built over the typical element after a typical element is isolated from the mesh.

We'll get the finite element model from the preceding equations (1) in this part by substituting finite element approximations of the following form:

$$\begin{aligned} S(t) &= \sum_{\ell=1}^{2} \bar{\mathbf{a}}_\ell \Upsilon_\ell, \qquad E(t) = \sum_{\ell=1}^{2} \bar{\mathbf{b}}_\ell \Upsilon_\ell, \qquad Q(t) = \sum_{\ell=1}^{2} \bar{\mathbf{c}}_\ell \Upsilon_\ell, \\ I_A(t) &= \sum_{\ell=1}^{2} \bar{\mathbf{d}}_\ell \Upsilon_\ell, \qquad I_S(t) = \sum_{\ell=1}^{2} \bar{\mathbf{e}}_\ell \Upsilon_\ell, \qquad R(t) = \sum_{\ell=1}^{2} \bar{\mathbf{f}}_\ell \Upsilon_\ell, \end{aligned} \tag{12}$$

together with

$$\phi_1 = \phi_2 = \phi_3 = \phi_4 = \phi_5 = \phi_6 = \Upsilon_\ell, \qquad (\ell = 1, 2).$$

In our calculations, we'll use two types of functions from a typical element (t_e, t_{e+1}), which are specified as follows:

Linear element:

$$\Upsilon_1^e = \frac{t_{e+1} - t}{t_{e+1} - t_e}, \qquad \Upsilon_2^e = \frac{t - t_e}{t_{e+1} - t_e}, \qquad t_e \leqq t \leqq t_{e+1}. \tag{13}$$

Quadratic element ($t_e \leqq t \leqq t_{e+1}$):

$$\Upsilon_1^e = \frac{(t_{e+1} - t_e - 2t)(t_{e+1} - t)}{(t_{e+1} - t_e)^2}, \quad \Upsilon_2^e = \frac{4(t - t_e)(t_{e+1} - t)}{(t_{e+1} - t_e)^2}, \quad \Upsilon_3^e = -\frac{(t_{e+1} - t_e - 2t)(t - t_e)}{(t_{e+1} - t_e)^2}. \tag{14}$$

By substituting the solution or element interpolation functions (12) into the aforementioned system (6)-(11), an approximate solution of the variational problem (6)-(11) is formed, and the element equations are formulated. The following matrix form (stiffness matrix) can be used to create the equations of the finite element model:

$$\begin{pmatrix} [K^{11}] & [K^{12}] & [K^{13}] & [K^{14}] & [K^{15}] & [K^{16}] \\ [K^{21}] & [K^{22}] & [K^{23}] & [K^{24}] & [K^{25}] & [K^{26}] \\ [K^{31}] & [K^{32}] & [K^{33}] & [K^{34}] & [K^{35}] & [K^{36}] \\ [K^{41}] & [K^{42}] & [K^{43}] & [K^{44}] & [K^{45}] & [K^{46}] \\ [K^{51}] & [K^{52}] & [K^{53}] & [K^{54}] & [K^{55}] & [K^{56}] \\ [K^{61}] & [K^{62}] & [K^{63}] & [K^{64}] & [K^{65}] & [K^{66}] \end{pmatrix} \begin{pmatrix} \{S\} \\ \{E\} \\ \{Q\} \\ \{IA\} \\ \{IS\} \\ \{R\} \end{pmatrix} = \begin{pmatrix} \{b^1\} \\ \{b^2\} \\ \{b^3\} \\ \{b^4\} \\ \{b^5\} \\ \{b^6\} \end{pmatrix}, \tag{15}$$

such that element matrices $[K^{rs}]$ and $[b^r]$ $(r, s = 1, 2, 3, 4, 5, 6,)$ are given by:

$$
\begin{aligned}
&[K_{ij}^{11}] = \int_{t_e}^{t_{e+1}} \left(\Upsilon_i \frac{d\Upsilon_j}{dt} + (\tau + \mu)\Upsilon_i \Upsilon_j \right) dt, \qquad [K_{ij}^{12}] = \beta \int_{t_e}^{t_{e+1}} (\Upsilon_i \, \bar{S} \, \Upsilon_j) \; dt,\\
&[K_{ij}^{13}] = 0, \qquad [K_{ij}^{14}] = 0, \qquad [K_{ij}^{15}] = 0, \qquad [K_{ij}^{16}] = 0,\\
&[K_{ij}^{21}] = -\beta \int_{t_e}^{t_{e+1}} (\Upsilon_i \, \bar{E} \, \Upsilon_j) \; dt, \qquad [K_{ij}^{22}] = \int_{t_e}^{t_{e+1}} \left(\Upsilon_i \frac{d\Upsilon_j}{dt} + (\gamma + \mu + \eta + \sigma)\Upsilon_i \Upsilon_j \right) dt,\\
&[K_{ij}^{23}] = 0, \qquad [K_{ij}^{24}] = 0, \qquad [K_{ij}^{25}] = 0, \qquad [K_{ij}^{26}] = 0,\\
&[K_{ij}^{31}] = -\tau \int_{t_e}^{t_{e+1}} (\Upsilon_i \, \Upsilon_j) \; dt, \qquad [K_{ij}^{32}] = -\gamma \int_{t_e}^{t_{e+1}} (\Upsilon_i \, \Upsilon_j) \; dt,\\
&[K_{ij}^{33}] = \int_{t_e}^{t_{e+1}} \left(\Upsilon_i \frac{d\Upsilon_j}{dt} + (\mu + \upsilon + \theta)\Upsilon_i \Upsilon_j \right) dt, \qquad [K_{ij}^{34}] = 0, \qquad [K_{ij}^{35}] = 0, \qquad [K_{ij}^{36}] = 0,\\
&[K_{ij}^{41}] = 0, \qquad [K_{ij}^{42}] = -\sigma \int_{t_e}^{t_{e+1}} (\Upsilon_i \, \Upsilon_j) \; dt, \qquad [K_{ij}^{43}] = -\theta \int_{t_e}^{t_{e+1}} (\Upsilon_i \, \Upsilon_j) \; dt,\\
&[K_{ij}^{44}] = \int_{t_e}^{t_{e+1}} \left(\Upsilon_i \frac{d\Upsilon_j}{dt} + (\mu + r_1)\Upsilon_i \Upsilon_j \right) dt, \qquad [K_{ij}^{45}] = 0, \qquad [K_{ij}^{46}] = 0,\\
&[K_{ij}^{51}] = 0, \qquad [K_{ij}^{52}] = -\eta \int_{t_e}^{t_{e+1}} (\Upsilon_i \, \Upsilon_j) \; dt, \qquad [K_{ij}^{53}] = -\upsilon \int_{t_e}^{t_{e+1}} (\Upsilon_i \, \Upsilon_j) \; dt,\\
&[K_{ij}^{54}] = 0, \qquad [K_{ij}^{55}] = \int_{t_e}^{t_{e+1}} \left(\Upsilon_i \frac{d\Upsilon_j}{dt} + (\delta - \mu - r_2)\Upsilon_i \Upsilon_j \right) dt, \qquad [K_{ij}^{56}] = 0,\\
&[K_{ij}^{61}] = 0, \qquad [K_{ij}^{62}] = 0, \qquad [K_{ij}^{63}] = 0, \qquad [K_{ij}^{64}] = -r_1 \int_{t_e}^{t_{e+1}} (\Upsilon_i \, \Upsilon_j) \; dt,\\
&[K_{ij}^{65}] = -r_2 \int_{t_e}^{t_{e+1}} (\Upsilon_i \, \Upsilon_j) \; dt, \qquad [K_{ij}^{66}] = \int_{t_e}^{t_{e+1}} \left(\Upsilon_i \frac{d\Upsilon_j}{dt} + \mu \, \Upsilon_i \Upsilon_j \right) dt,\\
&b_i^1 = \Lambda \int_{t_e}^{t_{e+1}} \Upsilon_i \, dt, \qquad b_i^2 = 0, \qquad b_i^3 = 0, \qquad b_i^4 = 0, \qquad b_i^5 = 0, \qquad b_i^6 = 0,
\end{aligned}
\tag{16}
$$

in which

$$
\bar{S} = \sum_{\ell=1}^{2} \bar{S}_\ell \Upsilon_\ell, \qquad \bar{E} = \sum_{\ell=1}^{2} \bar{E}_\ell \, \Upsilon_\ell.
$$

We compute all the integrals in (15) using Gaussian quadrature, so we can see that the applicability of the form functions varies from problem to problem. We use linear and quadratic shape functions to create a simple and efficient implementation in computations in the current problem. However, the results do not differ significantly, implying that both elements yield nearly the same accuracy.

4.3 Imposition of the boundary conditions and the solution of the algebraic equations system

1. We divide the entire domain into 700 line elements, and since each element matrix is of the order 12×12, we may construct a matrix of the order 8406×8406 by following the assembly of all of the element equations. We'll use an iterative technique to solve the resulting system

of equations because it's significantly nonlinear. By including the functions $\bar{S}$, and $\bar{E}$, which are assumed to be known, the system is linearized. After applying the supplied initial conditions, the resultant system will reduce to 8395 equations.

2. In order to solve this problem, we use the Gauss elimination method with a precision of 0.0001. The relative difference between the current and prior iterations is used as a convergence criterion. When the precision of these differences reaches the desired level, the solution is said to have converged, and the iterative process is over.

5 Numerical simulation

We look at the proposed system (1) with the following parameter values [23]:

$$\tau = 0.0002, \quad \beta = 0.0805, \quad \delta = 0.000016728, \quad \gamma = 0.00020138, \quad \eta = 0.4478, \quad \theta = 0.0101,$$

$$\mu = 0.0106, \quad \upsilon = 0.0003208, \quad \sigma = 0.0668, \quad \Lambda = 0.02537, \quad r1 = 0.00005734, \quad r2 = 0.00001673,$$

and different values of S_0, E_0, Q_0, IA_0, IS_0, R_0. Figures 2-4 show a numerical simulation of the investigated model using the proposed method.

Figure 2 depicts the behavior of the approximate solution for various natality rate values $\Lambda = 0.01, 0.03, 0.05$, in the interval $(0, 120)$, with initial conditions $S_0 = 0.5$, $E_0 = 0.2$, $Q_0 = 0.1$, $IA_0 = 0.2$, $IS_0 = 0.1$, $R_0 = 0.0$. Where in this case, the fundamental reproduction number $\mathfrak{R}_0 < 1$ in all cases, and in the view of Theorem 1, we can note that the disease free equilibrium point $\bar{\mathbf{E}}_0$ is locally asymptotically stable.

In Figure 3, we show the behavior of the approximate solution in the domain $(0, 120)$ where the components of solution $S(t)$, $E(t)$, $Q(t)$, $IA(t)$, $IS(t)$, $R(t)$ are represented by different values of the initial conditions in Figures 3a-3f, respectively. In this situation, we'll look at three scenarios:

i. $S_0 = 0.5$, $E_0 = 0.1$, $Q_0 = 0.1$, $IA_0 = 0.3$, $IS_0 = 0.3$, $R_0 = 0.0$;

ii. $S_0 = 0.3$, $E_0 = 0.2$, $Q_0 = 0.2$, $IA_0 = 0.1$, $IS_0 = 0.2$, $R_0 = 0.0$;

iii. $S_0 = 0.5$, $E_0 = 0.3$, $Q_0 = 0.3$, $IA_0 = 0.2$, $IS_0 = 0.1$, $R_0 = 0.0$.

In all of these circumstances, the fundamental reproduction number $\mathfrak{R}_0 < 1$ is used.

The residual error function (REF) is introduced in Figure 4 using the same parameters and domain as in Figure 2, as well as the following initial conditions:

$$S_0 = 0.5, \quad E_0 = 0.2, \quad Q_0 = 0.1, \quad IA_0 = 0.2, \quad IS_0 = 0.1, \quad R_0 = 0.0.$$

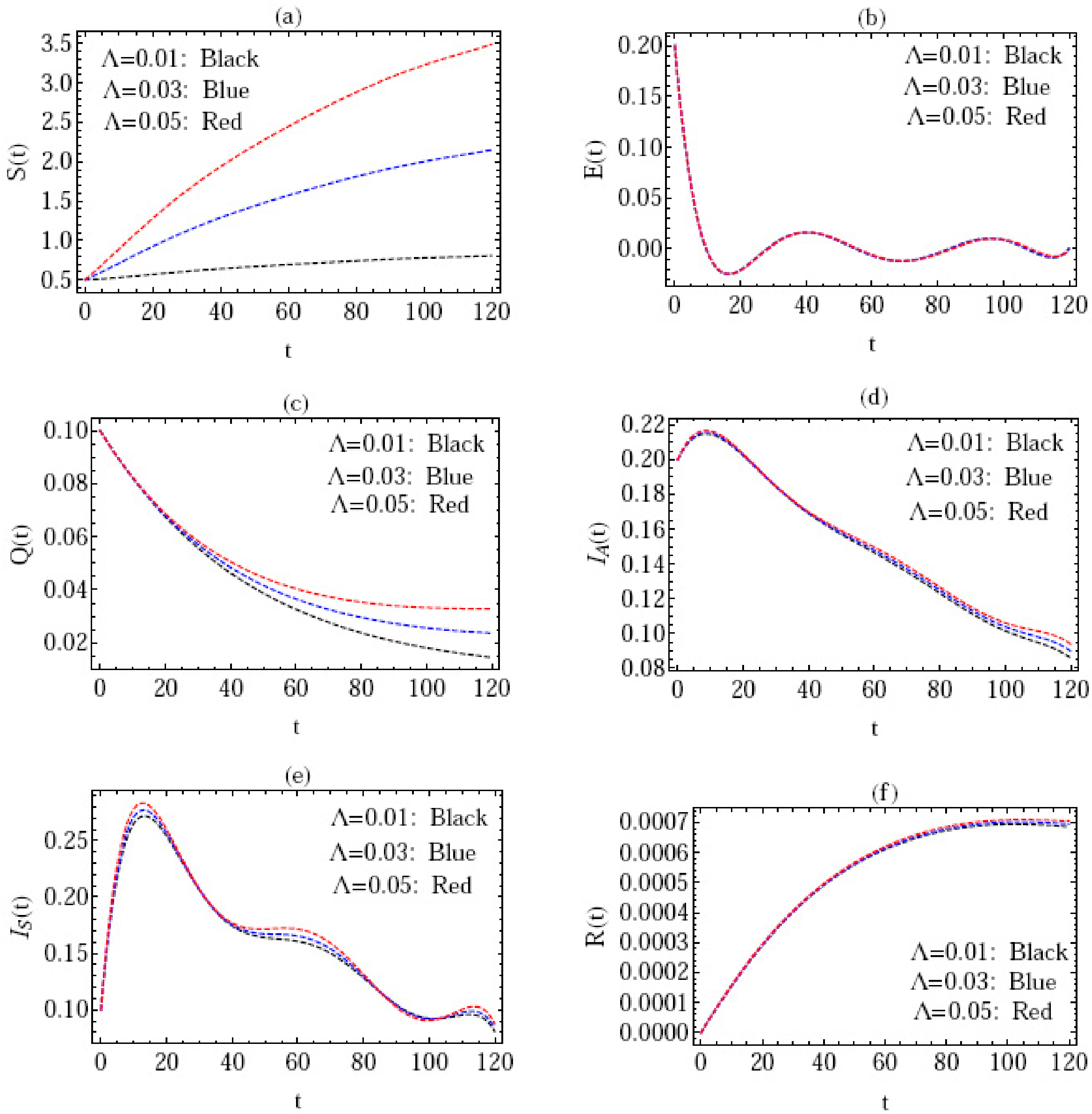

Figure 2. Behavior of the approximate solution via different values of Λ.

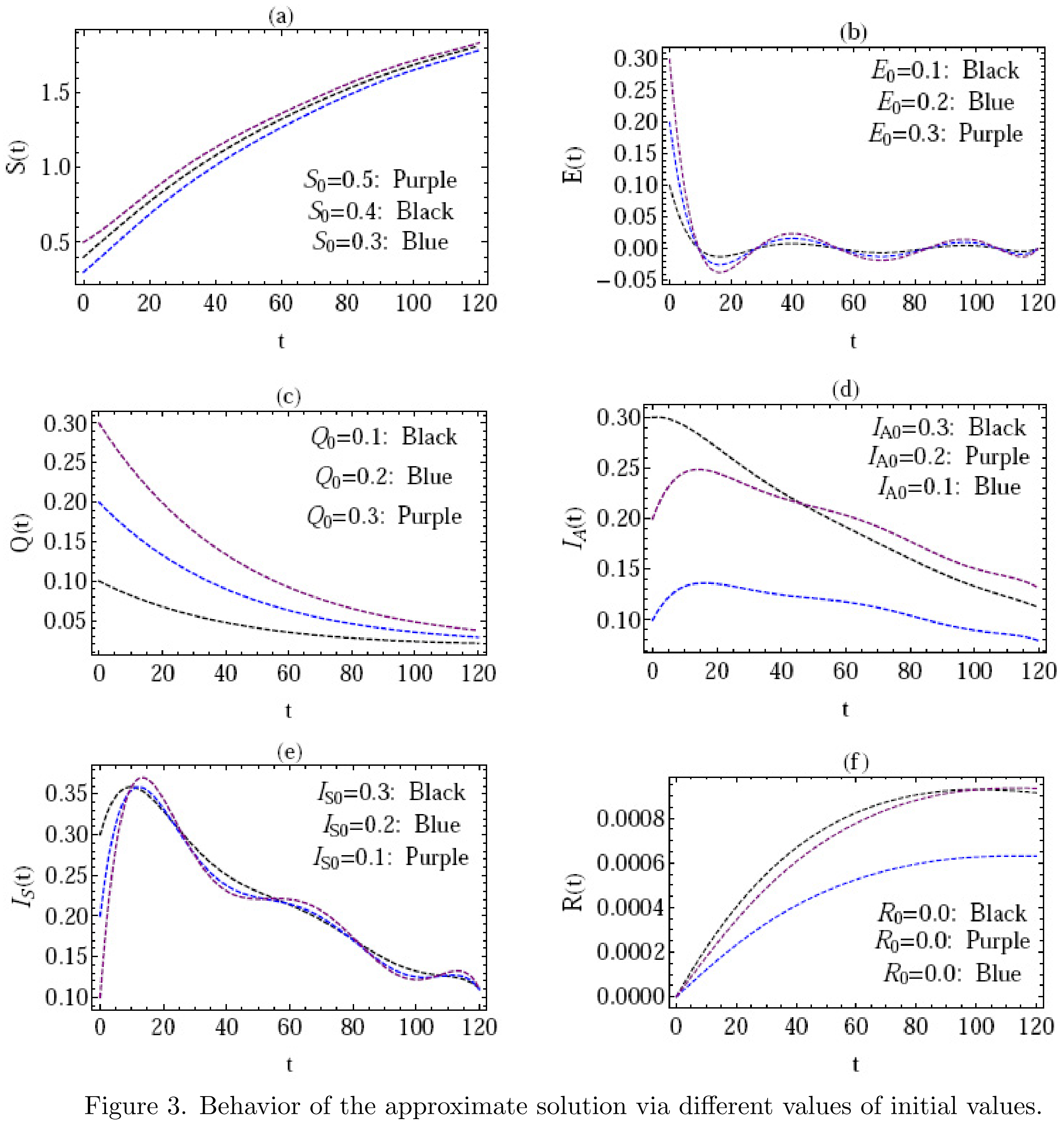

Figure 3. Behavior of the approximate solution via different values of initial values.

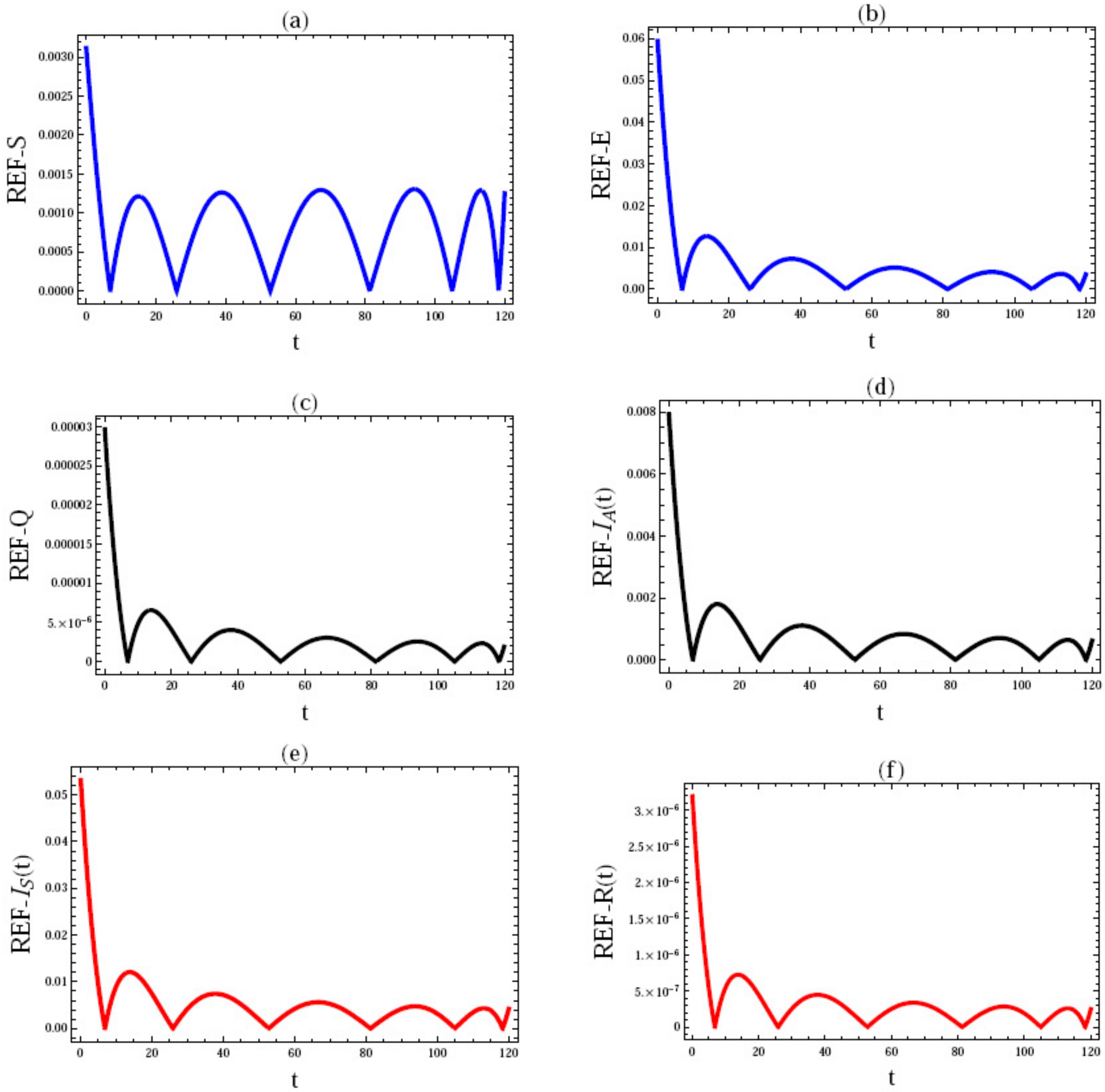

Figure 4. The REF of the approximate solution.

We can see from this figure that the theoretical results on stability acquired in the preceding section are correct.

We compared the solution generated by the FEM with the fourth-order Runge-Kutta method in Figure 5 (RK4) with the same parameters and domain $(0, 150)$ as in Figure 4, and the following initial conditions $S_0 = 0.2, \quad E_0 = 0.1, \quad Q_0 = 0.1, \quad IA_0 = 0.2, \quad IS_0 = 0.2, \quad R_0 = 0.0.$
The behavior of the numerical solution is dependent on the values of Λ, the initial circumstances, and the included parameters τ, β, δ, γ, η, θ, μ, υ, σ, Λ, r_1, r_2, as shown in Figures 2-5, indicating that the proposed approach is well implemented for solving the given problem. We may also validate that the disease's expected behavior has occurred, resulting in a clear simulation of the

model.

6 Conclusions and remarks

We used the FEM to simulate the proposed model (Covid-19) in this work. A specific emphasis is placed on presenting the qualitative analysis of the model. The model contains two equilibrium points: disease-free equilibrium point $\bar{\mathbf{E}}_0$ and endemic equilibrium point $\bar{\mathbf{E}}_1$, according to the findings. In addition, the equilibrium points reveal that $\bar{\mathbf{E}}_0$ is locally asymptotically stable whenever the fundamental reproduction number, $\mathfrak{R}_0 < 1$, and $\bar{\mathbf{E}}_1$ are globally asymptotically stable whenever $\mathfrak{R}_0 > 1$. The parameters in the $\mathfrak{R}_0$ were subjected to a sensitivity analysis, and the profile of each state variable was also presented using the fitted values of the parameters to demonstrate the disease's spread. The contact rate between susceptible individuals and the rate of transfer of persons from exposed to symptomatically infected classes are the most sensitive criteria in the $\mathfrak{R}_0$. The solutions obtained with various values for the parameters, as well as the initial conditions for the studied problem, demonstrate that the offered method is well suited to successfully explore this model. In addition, the REF is calculated to ensure that the suggested technique is genuine. The results approve that the given approach is an effective tool for investigating the numerical solution for such models. Finally, we can see that our numerical solution of the suggested model and the numerical solution obtained using the RK4 method are in perfect agreement. Our study, on the other hand, may provide stronger physical interpretations for future theoretical and computational investigation on this topic by capturing this numerical analysis. Mathematica is used to calculate all numerical results.

Availability of data and material:

All data generated or analyzed during this study are included in this published article.

Competing interests:

There are no competing interests declared by the authors.

Authors contributions:

This study was written in collaboration by all of the authors. The final manuscript was read and approved by all writers.

Acknowledgements:

The authors extend their appreciation to Princess Nourah bint Abdulrahman University for fund this research under Researchers Supporting Project number (PNURSP2023R229) Princess Nourah bint Abdulrahman University, Riyadh, Saudi Arabia

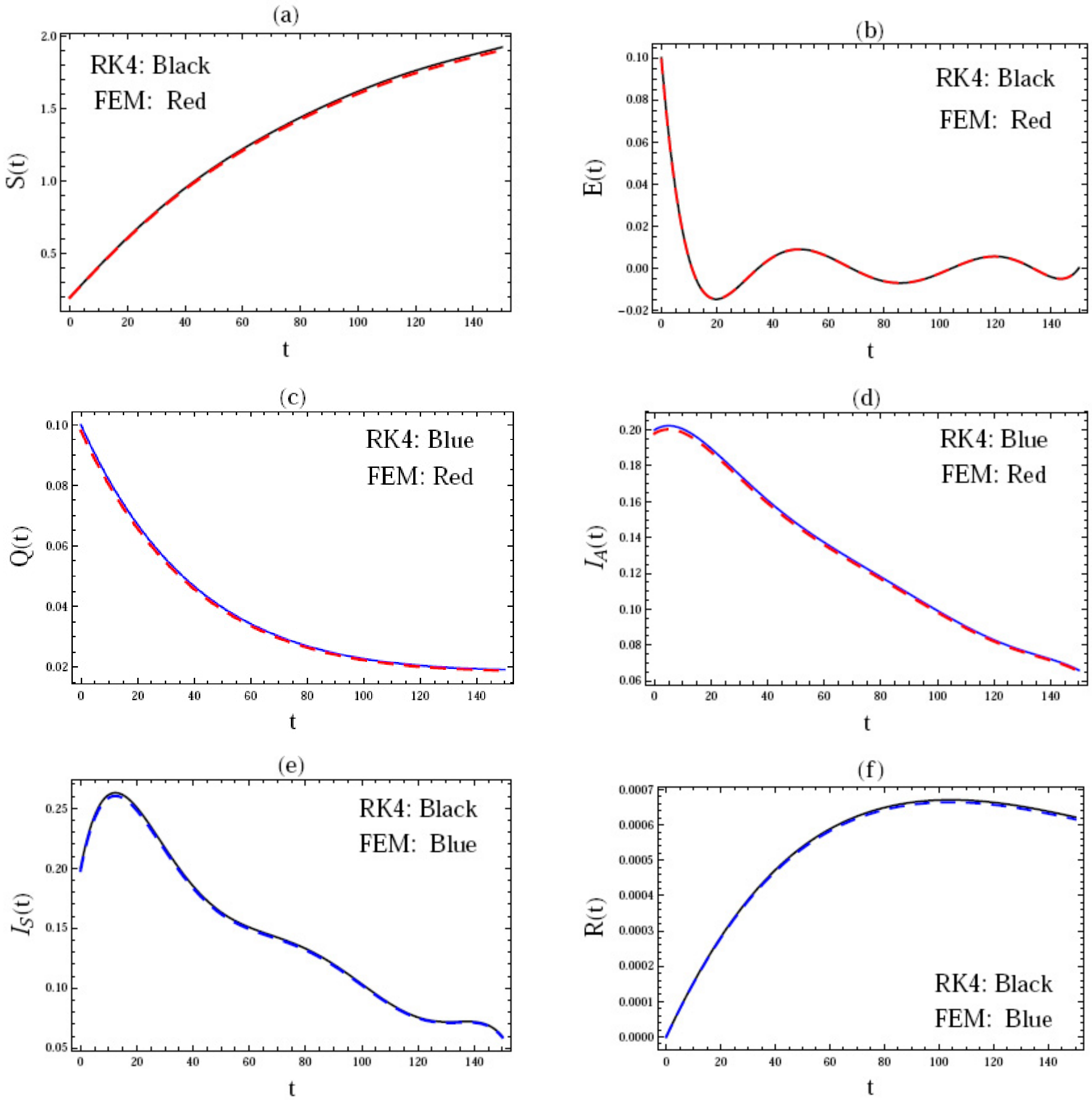

Figure 5. Comparison the solution obtained by FEM and RK4.

References

[1] R. M. Anderson and R. M. May, Helminth infections of humans: mathematical models, population dynamics, and control, *Advances in Parasitology*, **24**, p.(1-101), 1985.

[2] L. Edelstein-Keshet, Mathematical models in biology, *SIAM*, 2005.

[3] World health organization. novel coronavirus diseases 2019. URL: https://www.who.int/emergencies/diseases/novel-coronavirus-2019 [accessed: 2020-10-14].

[4] World health organization. report of the who-china joint mission on coronavirus disease 2019 (covid-19), february 2020. URL: https://www.who.int/docs/ defaultsource/coronaviruse/who-china-jointmission-on-covid-19-final-report.pdf [accessed: 2020-10-14].

[5] W. Ajisegiri, O. Odusanya and R. Joshi, Covid-19 outbreak situation in nigeria and the need for effective engagement of community health workers for epidemic response, *Global Biosecur*, **1(4)**, p.(5-20), 2020.

[6] D. Baud, X. Qi, K. Nielsen-Saine, K, D. Musso, L. Pomar and G. Favre, Real estimates of mortality following covid-19 infection, *Lancet Infect. Dis.*, **11**, p.(13-23), 2020.

[7] J. R. Koo, A. R. Cook, M. Park, Y. Sun, H. Sun, J. T. Lim, C. Tam and B. L. Dickens, Interventions to mitigate early spread of sarscov-2 in singapore: a modelling study, *Lancet Infect. Dis.,* **15**, 2020.

[8] O. A. Adegboye, A. I. Adekunle and E. Gayawan, Early transmission dynamics of novel coronavirus (covid-19) in Nigeria, *Int. J. Environ Res. Public Health*, **17(9)**, p.(10-25), 2020.

[9] S. B. Chen, S. Rashid, M. A. Noor, Z. Hammouch and Y. M. Chu, New fractional approaches for n-polynomial p-convexity with applications in special function theory, *Adv. Differ. Equ.,* **2020**, p.(11-31), 2020.

[10] J. Danane, K. Allali and Z. Hammouch, Mathematical analysis of a fractional differential model of HBV infection with antibody immune response, *Chaos Solitons Fract*, **136**, p.(1-11), 2020.

[11] M. A. Hajji and Q. Al-Mdallal, Numerical simulations of a delay model for immune system-tumor interaction, *Sultan Qaboos Univ. J. Sci.*, **23(1)**, p.(19-31), 2018.

[12] Y. F. Ibrahim, M. M. Khader, A. Megahed, F. Abd Elsalam and M. Adel, An efficient numerical simulation for the fractional Covid-19 model by using the GRK4M together with and the fractional FDM, *Fractal and fractional*, **6(304)** (2022) 1-14.

[13] M. M. Khader and M. Adel, Numerical approach for solving the Riccati and Logistic equations via QLM-rational Legendre collocation method, *Computational and Applied Mathematics,* **39(166)**, p.(1-9), 2020.

[14] M. M. Khader and M. Adel, Modeling and Numerical Simulation for Covering the Fractional Covid-19 Model Using Spectral Collocation-Optimization Algorithms, *Fractal and fractional*, **6(363)** (2022) 1-19.

[15] Y. Y. Lin and S. P. Lo, Finite element modeling for chemical mechanical polishing process under different back pressures, *J. Materials Process. Tech.*, **140**, p.(646-652), 2003.

[16] P. Rana and R. Bhargava, Flow and heat transfer of a nanofluid over a nonlinearly stretching sheet: A numerical study, *Commun. Nonlinear Sci. Numer. Simulat.*, **17**, p.(212-226), 2012.

[17] K. M. Saad, M. M. Khader, J. F. Gomez-Aguilar and Dumitru Baleanu, Numerical solutions of the fractional Fisher's type equations with Atangana-Baleanu fractional derivative by using spectral collocation methods, *Chaos,* **29**, p.(1-5), 2019.

[18] M. Adel, Numerical simulations for the variable order two-dimensional reaction sub-diffusion equation: Linear and nonlinear, *Fractals, Complex Geometry, Patterns, and Scaling in Natural and Society*, **30(1)**, 2022, manuscript Number 2240019.

[19] W. M. Abd-Elhameed and A. M. Alkerledri, Spectral solutions of linear and nonlinear BVPs using certain jacobi polynomials generalizing third- And fourth-kinds of chebyshev polynomials, *CMES - Computer Modeling in Fhgineering and Sciences*, **126(1)**, (2021) 1-35.

[20] A. Napoli, W. M. Abd-Elhameed, An innovative harmonic Aumbers operational matrix method for solving initial value problems, *Calcolo*, **54(1)**, (2017) 57-76.

[21] Y. H. Youssri and W. M. Abd-Elhameed, Numerical spectral Legendre-Galerkin algorithm for solving time fractional telegraph equation, *Romanian Journal of Physics*, **63(3-4)**, (2018) 107.

[22] M. Adel M, H. M. Srivastava and M. M. Khader, Implementation of an accurate method for the analysis and simulation of electrical R-L circuits, *Math Meth Appl Sci.,* **12** (2022) 1-10.

[23] I. Ahmed, G. U. Modu, A. Yusuf, P. Kumam, and I. Yusuf, A mathematical model of Coronavirus Disease (COVID-19) containing asymptomatic and symptomatic classes, *Results in Physics*, **21** p.(1-14), 2021.

[24] O. Diekmann, J. A. P. Heesterbeek and J. A. Metz, On the definition and the computation of the basic reproduction ratio R_0 in models for infectious diseases in heterogeneous populations, *J. Math. Biol.*, **28(4)**, p.(365-382), 1990.

[25] A. Hansbo and P. Hansbo, A finite element method for the simulation of strong and weak discontinuities in solid mechanics, Comput. Methods Appl. Mech. Engrg., **139**, p.(3523-3540), 2004.

[26] R. Bhargava, S. Sharma, H. S. Takhar, O. A. Beg and P. Bhargava, Numerical solutions for micropolar transport phenomena over a nonlinear stretching sheet, Nonlinear Anal: Model. Cont., **12**, p.(45-63), 2007.

[27] K. J. Bathe, Finite Element Procedures. Prentice Hall, Pearson Education Incorporated, New York, 2006.